Tech Science Press

Wave Propagation Model in a Human Long Poroelastic Bone under Effect of Magnetic Field and Rotation

A. M. Abd-Alla[1,*], Hanaa Abu-Zinadah[2], S. M. Abo-Dahab[3], J. Bouslimi[4,5] and M. Omri[6]

[1]Department of Mathematics, Sohag University, Sohag, Egypt
[2]Department of Statistics, University of Jeddah, College of Science, Jeddah, Saudi Arabia
[3]Department of Mathematics, South Valley University, Qena, 83523, Egypt
[4]Department of Engineering Physics and Instrumentation, National Institute of Applied Sciences and Technology, Carthage University, Tunisia
[5]Department of Physics, Taif University, Taif, Saudi Arabia
[6]Deanship of Scientific Research, King Abdulaziz University, Jeddah, Saudi Arabia
[*]Correspondence: A. M. Abd-Alla. Email: mohmrr@yahoo.com
Received: 10 June 2020; Accepted: 20 August 2020

Abstract: This article is aimed at describing the way rotation and magnetic field affect the propagation of waves in an infinite poroelastic cylindrical bone. It offers a solution with an exact closed form. The authors got and examined numerically the general frequency equation for poroelastic bone. Moreover, they calculated the frequencies of poroelastic bone for different values of the magnetic field and rotation. Unlike the results of previous studies, the authors noticed little frequency dispersion in the wet bone. The proposed model will be applicable to wide-range parametric projects of bone mechanical response. Examining the vibration of surface waves in rotating cylindrical, long human bones under the magnetic field can have an impact. The findings of the study are offered in graphs. Then, a comparison with the results of the literature is conducted to show the effect of rotation and magnetic field on the wave propagation phenomenon. It is worth noting that the results of the study highly match those of the literature.

Keywords: Propagation of waves; rotation; magnetic field; poroelastic; wet bone; natural frequency; magnetic field

1 Introduction

One of the highly considerable clinical methods for identifying the integrity of bones *in vivo* is radiographic examination, though, X-ray cannot detect when the loss of a bone decreases less than 30%. By the same token, periodic X-rays can always be utilized in monitoring the healing of fractures although evaluating the healing degree is subjective and often inaccurate. Natall et al. [1] examined bones as a material from a biomechanical perspective. The authors of [2–7] explored various issues related to the propagation of waves within poroelastic cylinders. In regard to a porous anisotropic solid, Biot [8] introduced the theory of elasticity and consolidation. In another study, Biot [9] discussed the theory of elastic wave propagation in a solid that is fluid-saturated and porous. Cardoso et al. [10] investigated the

role of the biological tissue structural anisotropy in the poroelastic propagation of waves. The authors of [11] solved issues related to the propagation of coupled poroelastic/acoustic/elastic waves through automatic hp-adaptively. In 3D poroelastic solids, Wen [12] used the meshless local Petrov–Galerkin method for the propagation of waves. Morin et al. [13] investigated the arduous multiscale poromicrodynamics method that is effective in the diverse bone tissues. Employing an iterative active medium approximation, Potsika et al. [14] introduced the model ultrasound propagation of waves in the healing of long bones. The authors of [15] analyzed theoretically the process of internal bone restoration motivated by a medullary pin. Nguyen et al. [16] investigated the performance of the flows of interstitial fluid in cortical bones controlled by axial cyclic harmonic loads that mimic the behavior of *in vivo* bones while doing daily activities, such as going for a walk. Misra et al. [17] derived the relation of dispersion for axisymmetric acoustic wave propagation along a long composite bone. Qin et al. [18] predicted theoretically the remodeling of the surface bone in the diaphysis of the long bone under different external loads controlled by the theory of adaptive elasticity. Mathieu et al. [19] studied biomechanically the performance of the bone-dental implant interface as an environmental task by taking into account the *in silico*, *in vivo*, and *ex vivo* projects on animal models. Brynk et al. [20] evaluated relevant experimental findings within a microporomechanic theoretical framework. Parnell et al. [21] compared the theoretical estimates of the active elastic moduli of cortical bone at the meso- and macroscales. Shah [22] studied the near-surface condition of stress established under the oscillatory contact between the artificial components that have a considerable role in defining fretting severity. Gilbert et al. [23] investigated the viscous interstitial fluid that plays a role in the ultrasound insonification of non-defatted cancellous bone. The authors of [24] solved analytically the noticeably long borehole in the isotropic and poroelastic medium inclined to the far-field principal stresses. Cowin [25] developed the interaction model of fluid and solid stages of a fluid-saturated porous medium. The effectiveness of bone healing in the ultrasonic reaction of the titanium implants that take the shape of coins and inserted in rabbit tibiae was discussed by Mathieu et al [26]. Singhal et al. [27] investigated the interior restoration of bone by defining the process that enables the bones to have the histological structure to modify within areas of long mechanical load. Kumha [28] investigated the shear wave in a primarily stressed poroelastic medium that has corrugated boundary surfaces inserted between a higher material strengthened with fiber and isotropic inhomogeneous half-space.

Abo-Dahab et al. [29] investigated the analytical solution for surface waves' remodeling in the long bones under the magnetic field and rotating. Farhan [30] discussed the effect of rotation on the propagation of waves in a hollow poroelastic circular cylinder with a magnetic field. Marin et al. [31] investigated the structural continuous dependence in micropolar porous bodies. Abo-Dahab et al. [32] discussed the effect of rotation on the propagation of waves model in a human long poroelastic bone.

In this paper, the way rotation and magnetic field affect the propagation of waves in an infinite poroelastic cylindrical bone is discussed. The paper provides a solution with an exact closed form. The authors got and examined numerically the general frequency equation of the poroelastic bone. Moreover, they calculated the frequencies of the poroelastic bone for different values of the magnetic field and rotation. Unlike the results of the previous studies, the authors noticed little frequency dispersion in the wet bone. The proposed model will be applicable to wide-range parametric projects of bone mechanical response. Examining the vibration of surface waves in rotating cylindrical, long human bones under the magnetic field can have an impact. The findings of the study are offered in graphs. Then, a comparison with the results of the literature is conducted. It is worth noting that the results of the study highly match those of the literature.

2 Formulation of the Problem

Take into account a hollow cylinder in the form of a geometric approximation to a long bone that is well-defined in the cylindrical coordinates r, θ, z. To carry out the analysis, assume the z-axis as the long bone

axis and a and b as the internal and external radius of the cortical thickness, respectively. Moreover, the linear theory of transverse isotropy that is effective for small strain provides the resulting stress-displacement and velocity relationships in the following form

$$\tau_{rr} = c_{11} \frac{\partial u_r}{\partial r} + c_{12} r^{-1} \left(u_r + \frac{\partial u_\theta}{\partial \theta} \right) + c_{13} \frac{\partial u_z}{\partial z} + M \left[\frac{\partial v_r}{\partial r} + r^{-1} \left(v_r + \frac{\partial v_\theta}{\partial \theta} \right) + \frac{\partial v_z}{\partial z} \right],$$

$$\tau_{\theta\theta} = c_{12} \frac{\partial u_r}{\partial r} u_r + c_{11} r^{-1} \left(u_r + \frac{\partial u_\theta}{\partial \theta} \right) + c_{13} \frac{\partial u_z}{\partial z} + M \left[\frac{\partial v_r}{\partial r} + r^{-1} \left(v_r + \frac{\partial v_\theta}{\partial \theta} \right) + \frac{\partial v_z}{\partial z} \right],$$

$$\tau_{zz} = c_{13} \left[\frac{\partial u_r}{\partial r} + r^{-1} \left(u_r + \frac{\partial u_\theta}{\partial \theta} \right) \right] + c_{33} \frac{\partial u_z}{\partial z} + Q \left[\frac{\partial v_r}{\partial r} + r^{-1} \left(v_r + \frac{\partial v_\theta}{\partial \theta} \right) + \frac{\partial v_z}{\partial z} \right],$$

$$\tau_{rz} = c_{44} \left[\frac{\partial u_z}{\partial r} + \frac{\partial u_r}{\partial z} \right],$$

$$\tau_{r\theta} = c_{66} \left[\frac{\partial u_\theta}{\partial r} + r^{-1} \left(D_\theta^\alpha u_r - u_\theta \right) \right],$$ (1)

$$\tau_{\theta z} = c_{44} \left[\frac{\partial u_\theta}{\partial z} + r^{-1} \frac{\partial u_z}{\partial \theta} \right],$$

$$\tau = M \left[\frac{\partial u_r}{\partial r} + r^{-1} (u_r + \frac{\partial u_\theta}{\partial \theta}) \right] + Q \frac{\partial v_z}{\partial z} + R \left[\frac{\partial v_r}{\partial r} + r^{-1} \left(v_r + \frac{\partial v_\theta}{\partial \theta} \right) + \frac{\partial v_z}{\partial z} \right],$$

$$\sigma_{rr} = \mu_e H_0^2 (\frac{\partial u_r}{\partial r} + \frac{1}{r} u_r + \frac{\partial u_z}{\partial z})$$ (2)

where τ_{ij} acts as the solid stress, τ represents the fluid stress, and σ_{rr} is the magnetic stress. Additionally, c_{ij}, M, Q, R and $c_{66} = \frac{1}{2}(c_{11} - c_{12})$ represent the elastic constants.

The equation of the fluid is

$$b_{rr}^{-1} \nabla^2 \tau + b_{zz}^{-1} \nabla^2 \tau_{zz} = \frac{\partial(\varepsilon - \tau)}{\partial t}$$ (3)

where $b_{rr} = \mu f^2 / k_{rr}, b_{zz} = \mu f^2 / k_{zz}, \nabla^2$ represent the Laplacian operator in cylindrical coordinates, μ represents the viscosity, f represents the porosity, and k_{rr} and k_{zz} represent the permeability of the medium. The displacements of solid and velocity of fluid are represented by u_i and v_i, respectively. Moreover, the strains are given in displacement in the following form:

$$e_{ij} = \frac{1}{2} \left(u_{i,j} + u_{j,i} \right)$$ (4)

The dilation $e = u_{i,j}$ and $\epsilon = v_{i,i}$.

The motion equations are

$$\frac{\partial \tau_{rr}}{\partial r} + r^{-1} \frac{\partial \tau_{r\theta}}{\partial \theta} + \frac{\partial \tau_{rz}}{\partial z} + r^{-1}(\tau_{rr} - \tau_{\theta\theta}) + \mu_e H_0^2 \left(\frac{\partial^2 u_r}{\partial r^2} + \frac{1}{r} \frac{\partial u_r}{\partial r} - \frac{1}{r^2} u_r + \frac{\partial^2 u_z}{\partial r \partial z} \right) = \rho \left(\frac{\partial^2 u_r}{\partial r^2} - \Omega^2 u_r \right)$$

$$\frac{\partial \tau_{r\theta}}{\partial r} + r^{-1} \frac{\partial \tau_{\theta\theta}}{\partial \theta} + \frac{\partial \tau_{\theta z}}{\partial z} + 2r^{-1} \tau_{\theta r} = \rho \frac{\partial^2 u_\theta}{\partial t^2}$$ (5)

$$\frac{\partial \tau_{rz}}{\partial r} + r^{-1} \frac{\partial \tau_{\theta z}}{\partial \theta} + \frac{\partial \tau_{zz}}{\partial z} + r^{-1} \tau_{rz} + \mu_e H_0^2 \left(\frac{\partial^2 u_r}{\partial r \partial z} + \frac{\partial^2 u_z}{\partial z^2} - \frac{1}{r^2} \frac{\partial^2 u_z}{\partial \theta \partial z} \right) = \rho \left(\frac{\partial^2 u_r}{\partial r^2} - \Omega^2 u_z \right)$$

where ρ is the density, $\overrightarrow{\Omega} = (0, \Omega, 0)$ represents the rotation vector, H_0 represents the magnetic field, and t represents the time.

Replacing from Eq. (1) into Eq. (5), the result becomes

$$(c_{11} + \mu_e H_0^2) \left[\frac{\partial^2 u_r}{\partial r^2} + r^{-1} \frac{\partial u_r}{\partial r} - r^{-2} u_r \right] + \frac{r^{-2}(c_{11} - c_{12})}{2} \frac{\partial^2 u_r}{\partial \theta^2} + (c_{44} + \mu_e H_0^2) \frac{\partial^2 u_r}{\partial z^2} +$$

$$+ \frac{r^{-1}}{2}(c_{11} + c_{12}) \frac{\partial^2 u_\theta}{\partial r \partial \theta} - \frac{3r^{-2}}{2}(c_{11} - c_{12}) \frac{\partial u_\theta}{\partial \theta} + (c_{13} + c_{44} + \mu_e H_0^2) \frac{\partial^2 u_z}{\partial r \partial z} +$$

$$+ M \left[\frac{\partial^2 v}{\partial r^2} + r^{-1} \frac{\partial v}{\partial r} - r^{-2} v_r + r^{-1} \frac{\partial^2 v \theta}{\partial r \partial \theta} + \frac{\partial^2 v_z}{\partial r \partial z} \right] = \rho \left(\frac{\partial^2 u_r}{\partial t^2} - \Omega^2 \right),$$

$$\frac{r^{-1}}{2}(c_{11} + c_{12}) \frac{\partial^2 u_r}{\partial r \partial \theta} + \frac{3r^{-2}}{2}(c_{11} - c_{12}) \frac{\partial u_r}{\partial \theta} + \frac{1}{2}(c_{11} - c_{12}) \left[\frac{\partial^2 u_\theta}{\partial r \partial \theta} + r^{-1} \frac{\partial u_\theta}{\partial r} - r^{-2} u_\theta \right] +$$

$$+ r^{-2} c_{11} \frac{\partial^2 u_\theta}{\partial \theta^2} + c_{44} \frac{\partial^2 u_\theta}{\partial z^2} + r^{-1}(c_{13} + c_{44}) \frac{\partial^2 u_z}{\partial \theta \partial z} + r^{-1} \left[\frac{\partial^2 v}{\partial r^2} + r^{-1} \frac{\partial v}{\partial r} - r^{-2} v_r + r^{-1} \frac{\partial^2 v \theta}{\partial r \partial \theta} + \right. \quad (6)$$

$$\left. + \frac{\partial^2 v_z}{\partial r \partial z} \right] = \rho \frac{\partial^2 u_\theta}{\partial t^2}$$

$$(c_{13} + c_{44} + \mu_e H_0^2) \left[\frac{\partial^2 u_r}{\partial r \partial z} + r^{-1} \frac{\partial u_r}{\partial z} \right] + r^{-1}(c_{13} + c_{44}) \frac{\partial^2 u_\theta}{\partial \theta \partial z} + (c_{44} + \mu_e H_0^2) \left[\frac{\partial^2 u_r}{\partial r^2} + r^{-1} \frac{\partial u_r}{\partial r} - \right.$$

$$\left. - r^{-2} \frac{\partial^2 u_z}{\partial \theta^2} \right] + + (c_{44} + \mu_e H_0^2) \frac{\partial^2 u_z}{\partial z^2} + Q \left[\frac{\partial^2 v}{\partial r^2} + r^{-1} \frac{\partial v}{\partial r} - r^{-2} v_r + r^{-1} \frac{\partial^2 v \theta}{\partial r \partial \theta} + \frac{\partial^2 v_z}{\partial r \partial z} \right] = \quad (7)$$

$$= \rho \left(\frac{\partial^2 u_z}{\partial t^2} - \Omega^2 \right)$$

3 The Solution to the Problem

To obtain a solution to Eq. (7), use the following solution in the field equations

$$u_r = (\phi_{,r} + r^{-1} \psi_{,\theta}) e^{i(kz - \omega t)}, \qquad v_r = -\eta_{,r} e^{i(kz - \omega t)},$$

$$u_\theta = (r^{-1} \phi_{,\theta} - \psi_{,r}) e^{i(kz - \omega t)}, \qquad v_\theta = -\frac{1}{r} \eta_{,\theta} e^{i(kz - \omega t)}, \qquad (8)$$

$$u_z = \frac{i\omega}{h} e^{i(kz - \omega t)}, \qquad v_z = -ik\eta e^{i(kz - \omega t)}$$

where u_r, u_θ, u_z, v_r, v_θ and v_z represent the displacement components and velocity components, ω is the angular frequency, k represents the wavenumber, and $h = b - a$ represents the thickness of the cylinder. Additionally, a represents the inner radius; b represents the outer radius; ϕ, ψ, and η represent the displacement potentials introduced for solving the field Eq. (8).

Replacing from Eq. (1) into Eqs. (3) and (5) and using Eqs. (6) and (7), the following equations are obtained:

$$[(c_{44} + \mu_e H_0^2) \nabla^2 + \rho(\omega^2 - \Omega^2) - k^2(c_{44} - \mu_e H_0^2)] \phi - (c_{44} + c_{13} + \mu_e H_0^2) \frac{kw}{h} - M(\nabla^2 - k^2) \eta = 0,$$

$$[(c_{44} + \mu_e H_0^2) \nabla^2 + \rho(\omega^2 - \Omega^2) - k^2 c_{33}] \frac{w}{h} + (c_{13} + c_{44} + \mu_e H_0^2) k \nabla^2 \phi + kQ(\nabla^2 - k^2) \eta = 0,$$

$$[M(b_{rr}^{-1} \nabla - k^2 b_{zz}^{-1} \nabla^2) + i\omega \nabla^2] \phi + [\frac{Q}{h}(-kb_{rr}^{-1} \nabla^2 + k^3 b_{zz}^{-1}) - \frac{ik\omega}{h}] w + [R(-b_{rr}^{--1} \nabla^2 (\nabla^2 - k^2) + \quad (9)$$

$$+ b_{zz}^{-1} k^2 (\nabla^2 - k^2)) + i\omega(\nabla^2 - k^2)] \eta = 0,$$

$$[\frac{1}{2}(c_{11} - c_{12} + \mu_e H_0^2) \nabla^2 + \rho(\omega^2 - \Omega^2) - k^2(c_{44} - \mu_e H_0^2)] \psi = 0.$$

Introducing the parameter as $r = \dfrac{r}{h}$, $\varepsilon_1 = kh$ and $\omega = k\varsigma$, Eq. (9) takes a dimensionless form as

$$[(\bar{c}_{11} + \mu_e H_0^2) + (ch)^2 - \varepsilon_1^2]\phi - (\bar{c}_{13} + 1)\varepsilon_1 w - M\xi = 0,$$
$$(\bar{c}_{13} + 1)\varepsilon_1 \nabla^2 \phi + (\nabla^2 + (ch)^2 - \varepsilon_1^2 \bar{c}_{33})w - \varepsilon_1 \overline{Q}\xi = 0, \tag{10}$$
$$\nabla^2(\nabla^2 - b\varepsilon_1^2 + i\overline{D})\phi - \varepsilon_1(Q'\nabla^2 + bQ'\varepsilon_1^2 - i\overline{D})w + (-R'\nabla^2 + bR'\varepsilon_1^2 + i\overline{D})\xi = 0.$$

$$(c_{66}\nabla^2 + (ch)^2 - \varepsilon_1^2)\psi = 0. \tag{11}$$

where

$$\xi = (\nabla^2 - \varepsilon_1^2)\eta, \quad \overline{D} = \frac{\omega h^2 b_{rr}}{M}, \quad R' = \frac{R}{M}, \quad \overline{M} = \frac{M}{c_{44} + \mu_e H_0^2}, \quad \overline{Q} = \frac{Q}{c_{44} + \mu_e H_0^2},$$

$$c^2 = \frac{\rho(\omega^2 - \Omega^2)}{c_{44} + \mu_e H_0^2}, b = \frac{b_{rr}}{b_{zz}}, \quad \bar{c}_{ij} = \frac{c_{ij}}{c_{44}} \quad (i,j = 1,2,3), \quad \nabla^2 = \frac{\partial^2}{\partial r^2} + r^{-1}\frac{\partial}{\partial r} + r^{-2}\frac{\partial^2}{\partial \theta^2}, \tag{12}$$

Because the fluid flow through the bone boundaries does not happen while exploring the wave propagation, ξ is defined in the above-mentioned form and it is not solved for the variable η. Though, when prescribing the flow on these boundaries, η may be estimated. Eq. (10) takes a determinant form as:

$$\begin{vmatrix} ((c_{11} + \mu_e|H_0^2)\nabla^2 + A) & -B & \overline{M} \\ B\nabla^2 & (\nabla^2 + C) & -\overline{Q}\varepsilon_1 \\ T_1 & T_2 & T_3 \end{vmatrix} (\phi, \zeta, \xi) = 0 \tag{13}$$

where

$$T_1 = \nabla^2(\nabla^2 - b + iD), \qquad T_2 = -\varepsilon_1(Q'\nabla^2 + bQ'\varepsilon^2 - iD),$$

$$T_3 = -(R'\nabla^2 + bR'\varepsilon_1^2 + iD), \qquad A = (ch)^2\varepsilon_1^2$$

$$\overline{B} = (1 + \bar{c}_{13})\varepsilon_1 \text{ and } C = (ch)^2 - \varepsilon_1^2\bar{c}_{13}$$

Estimating the determinant form, we have these equations:

$$(\nabla^6 + P\nabla^4 + G\nabla^2 + H)(\phi, w, \xi) = 0 \tag{14}$$

where

$$P = [R'\varepsilon_1^2(\bar{c}_{11} + \mu_e H_0^2) + iD(\bar{c}_{11} + \mu_e H_0^2) + CR'(\bar{c}_{11} + \mu_e H_0^2) - \overline{Q}Q'\varepsilon_1^2(\bar{c}_{11} + \mu_e H_0^2) + AR' - B^2R' +$$
$$+ BQ'\varepsilon_1 + \overline{M}\varepsilon_1^2 - \overline{Q}\varepsilon_1 B + i\overline{M}D + \overline{M}D]/(-R'(\bar{c}_{11} + \mu_e H_0^2) + \overline{M})),$$

$$G = [(\bar{c}_{11} + \mu_e H_0^2)(CR'\varepsilon_1^2 + iDC + Q'\varepsilon_1^4\overline{Q} - iD\overline{Q}\varepsilon_1^2) + AR'\varepsilon_1^2 + iDA + AR'C - AQ'\overline{Q}\varepsilon_1^2 +$$
$$+ BD\varepsilon_1^3 - iD\varepsilon_1 + C\varepsilon_1^3 - B\overline{Q}\varepsilon_1^3 + iDB\varepsilon_1\overline{M} + iDC\overline{M} - \overline{M}C\varepsilon_1^2]/(-R'(\bar{c}_{11} + \mu_e H_0^2) + \overline{M}),$$

$$H = -A(CR'\varepsilon_1^2 + iDC + \overline{Q}Q'\varepsilon_1^4 - iD\overline{Q}\varepsilon_1^2)/(R'(\bar{c}_{11} + \mu_e H_0^2) + \overline{M}).$$

The solution of Eq. (10) are

$$\phi = \sum_{i=1}^{3}[A_i J_n(\alpha_i x) + B_i Y_n(\alpha_i x)]con(n\theta),$$

$$w = \sum_{i=1}^{3} d_i[A_i J_n(\alpha_i x) + B_i Y_n(\alpha_i x)]con(n\theta), \tag{15}$$

$$\xi = \sum_{i=1}^{3} e_i[A_i J_n(\alpha_i x) + B_i Y_n(\alpha_i x)]con(n\theta)$$

where α_i^2 are the roots of the following equation

$$\alpha^6 - P\alpha^4 + G\alpha^2 - H = 0 \tag{16}$$

$$\alpha_1^2 = \frac{P}{3} - \frac{\sqrt[3]{2}(3G - P^2)}{3F1} + \frac{F_1}{3\sqrt{32}},$$

$$\alpha_2^2 = \frac{P}{3} + \frac{(1 + i\sqrt{3})(3G - P^2)}{\sqrt[3]{32}F1} - \frac{(1 - i\sqrt{3})F_1}{\sqrt[3]{62}},$$

$$\alpha_3^2 = \frac{P}{3} + \frac{(1 - i\sqrt{3})(3G - P^2)}{\sqrt[3]{1024}F1} - \frac{(1 - i\sqrt{3})F_1}{\sqrt[3]{62}}.$$

where

$F_1 = (27H - 9GP + 2P^3 + 3\sqrt{3}\sqrt{4G^3 + 27H^2 - 18GHP + 4HP^3})^{\frac{1}{3}}$ and d_i and e_i are calculated from the following equation

$$[(1 + \overline{c}_{11})\varepsilon_1 d_i + \overline{M}e_i = (\overline{c}_{11} + \mu_e H_0^2)\alpha_i^2 - (ch)^2 - \varepsilon_1^2],$$
$$(-\alpha_i^2 + (ch)^2 - \varepsilon_1^2 \overline{c}_{33})d_i - \overline{Q}\varepsilon_1 e_i = (1 + \overline{c}_{13})\varepsilon_1 \alpha_i^2. \tag{17}$$

The solution of Eq. (11) is

$$\psi = [A_4 J_n(\alpha_4 x) + B_4 Y_n(\alpha_4 x)] \sin(n\theta), \tag{18}$$

where

$$\alpha_4^2 = 2((ch)^2 - \varepsilon_1^2)/(\overline{c}_{11} + \mu_e H_0^2 - \overline{c}_{13}).$$

4 Frequency Equation

To have the boundary conditions that are free of traction, stress must disappear on the internal and external surfaces of the hollow cylinder, as follows:

$$\tau_{rr} + \sigma_{rr} = \tau_{rz} = \tau_{r\theta} = \tau = 0 \quad at \ r = a$$

$$\tau_{rr} + \sigma_{rr} = \tau_{rz} = \tau_{r\theta} = \tau = 0 \quad at \ r = b \tag{19}$$

where

$$\overline{a} = \frac{a}{h}, \quad \overline{b} = \frac{b}{h}.$$

Eqs. (8), (15) and (18) together with Eq. (19) and combining $A_1, B_1, A_2, B_2, A_3, B_3$ and A_4, B_4 coefficients help determine the characteristic frequency equation:

$$|a_{ij}| = 0, \quad i, j = 1, 2, 3, ..., 8 \tag{20}$$

where the coefficients of a_{ij} are given the form in the appendix.

The roots of Eq. (20) afford the curves of dispersion of the guided modes, namely the wavenumber as a frequency function.

$\rho = 0.1\_, 0.2\ldots, 0.3--, 0.4\_.\ \ \omega = 1\_, 1.1\ldots, 1.2--, 1.3\_.\ \ h = 0.1\_, 0.11\ldots, 0.12--, 0.13\ \ \ H_0 = 0.1\_\_, 0.3\ldots, 0.5--, 0.7\_.\_$
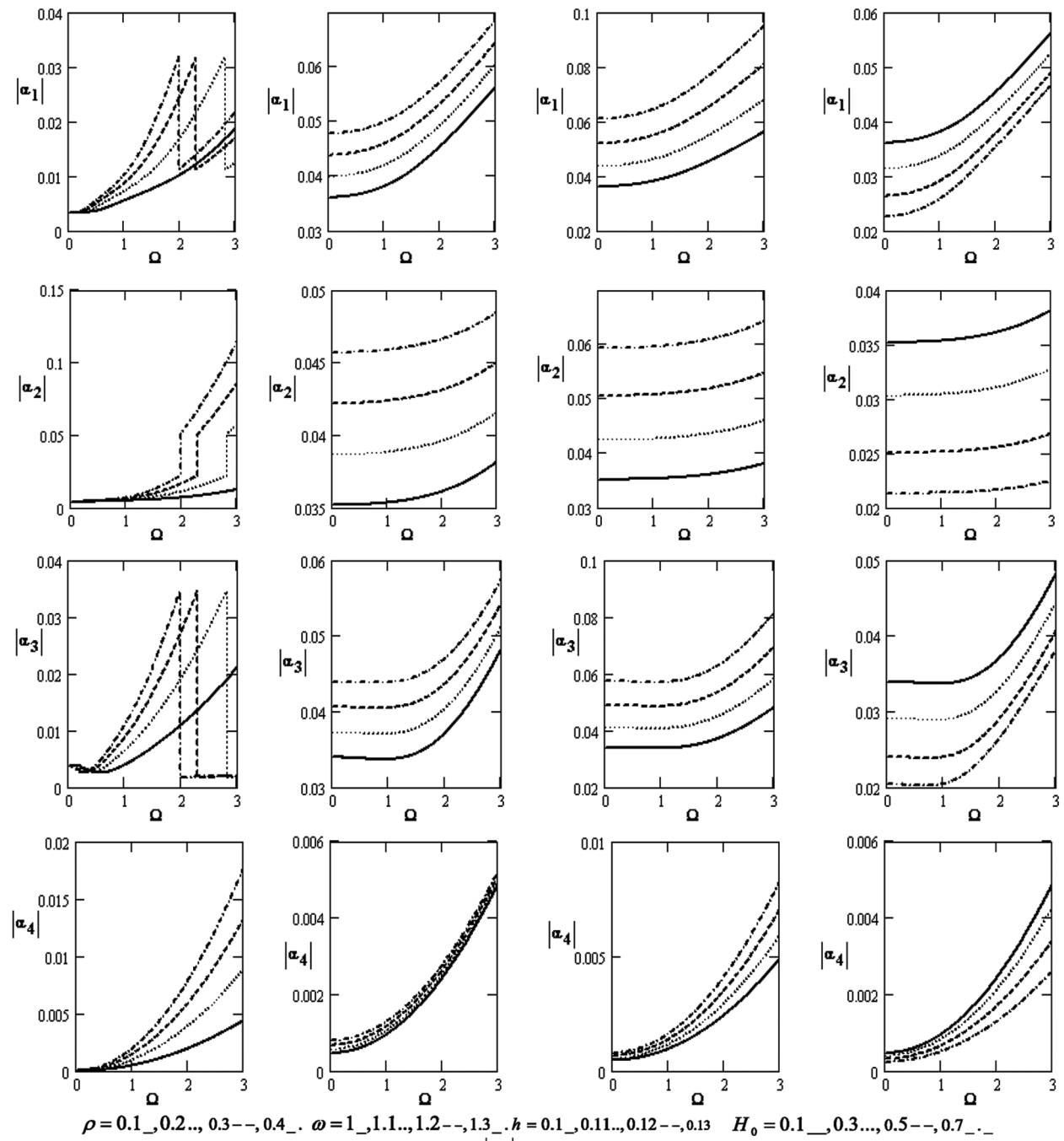
Figure 1: Variations of the roots $|\alpha_j|$ $(j = 1, 2, 3, 4)$ concerning the rotation Ω with different values for $\rho,\ \omega, h$ and H_0

$\rho = 0.1\_, 0.2.., 0.3--, 0.4\_.$ $\omega = 1\_, 1.1.., 1.2--, 1.3\_.$ $h = 0.1\_, 0.11.., 0.12--, 0.13$ $H_0 = 0.1\_, 0.3.., 0.5--, 0.7\_.$
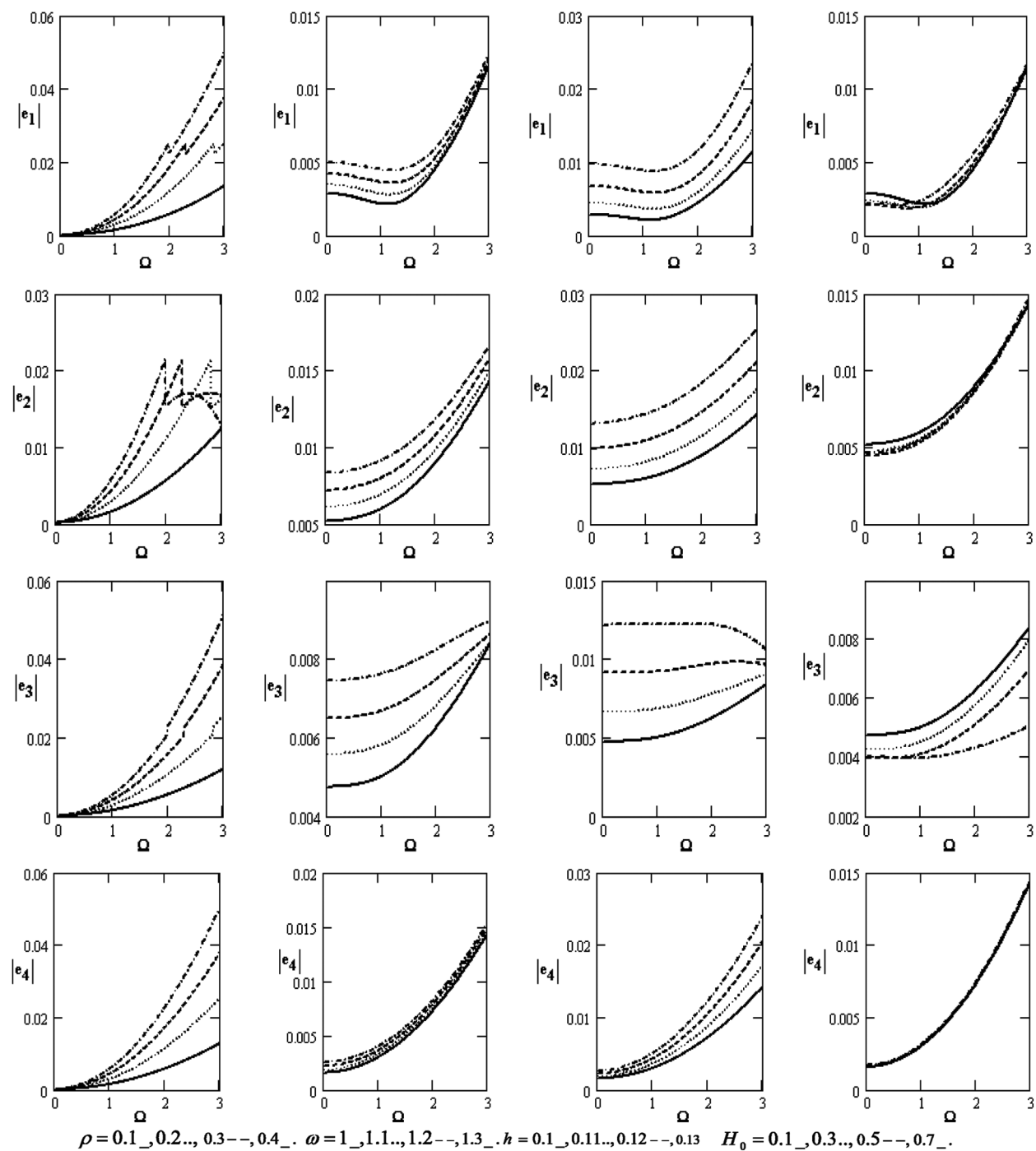
Figure 2: Variations of $|e_j|(j = 1, 2, 3, 4)$ with respect to the rotation Ω with different values for ρ, ω, h and H_0

$\rho = 0.1\_\_, 0.2.., 0.3--, 0.4\_.$ $\omega = 1\_\_, 1.1.., 1.2--, 1.3\_.$ $h = 0.1\_\_, 0.11.., 0.12--, 0.13$ $H_0 = 0.1\_\_, 0.3..., 0.5--, 0.7\_._$
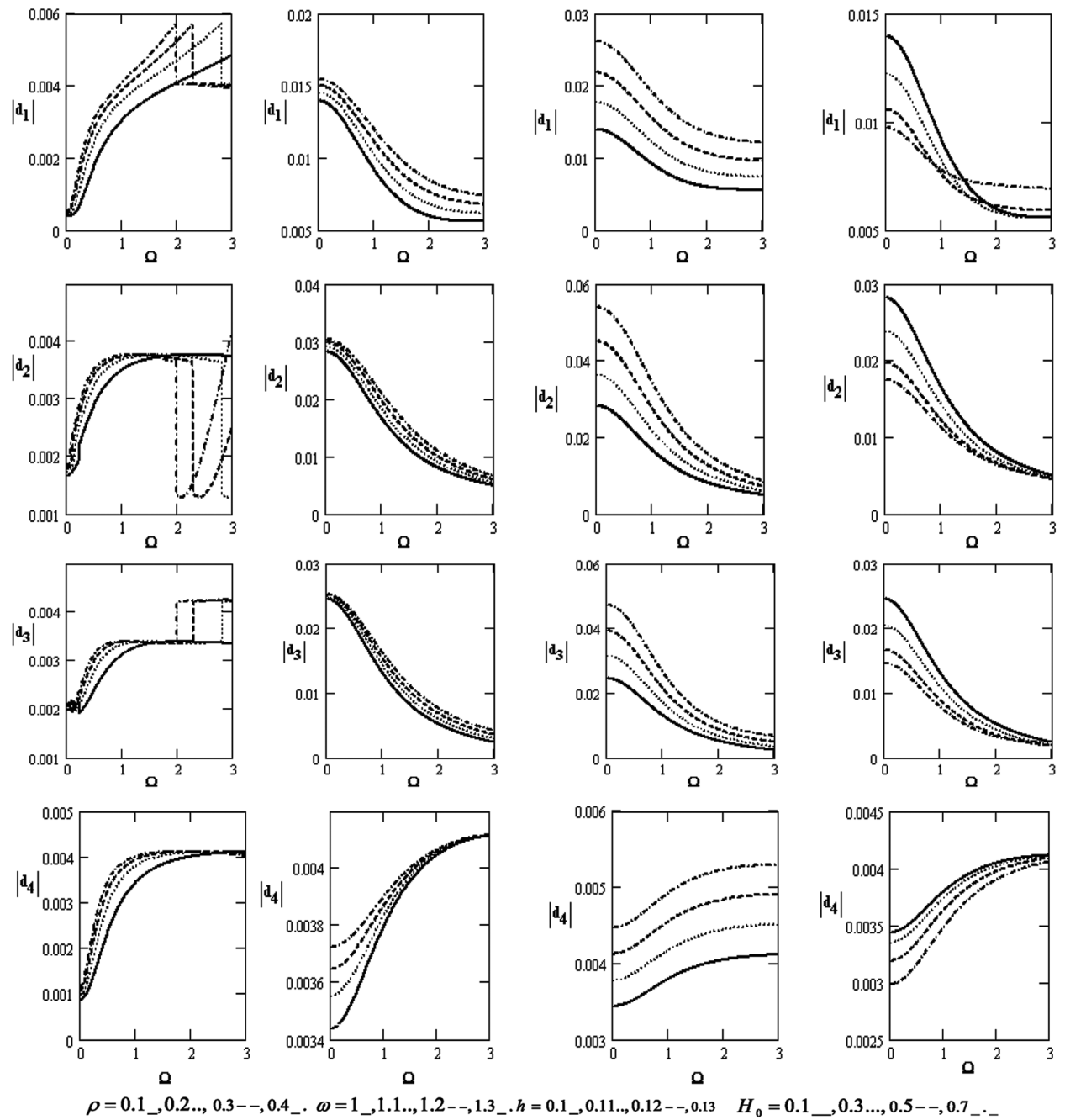
Figure 3: Variations of $|d_j|(j = 1, 2, 3, 4)$ concerning the rotation Ω with different values for ρ, ω, h and H_0
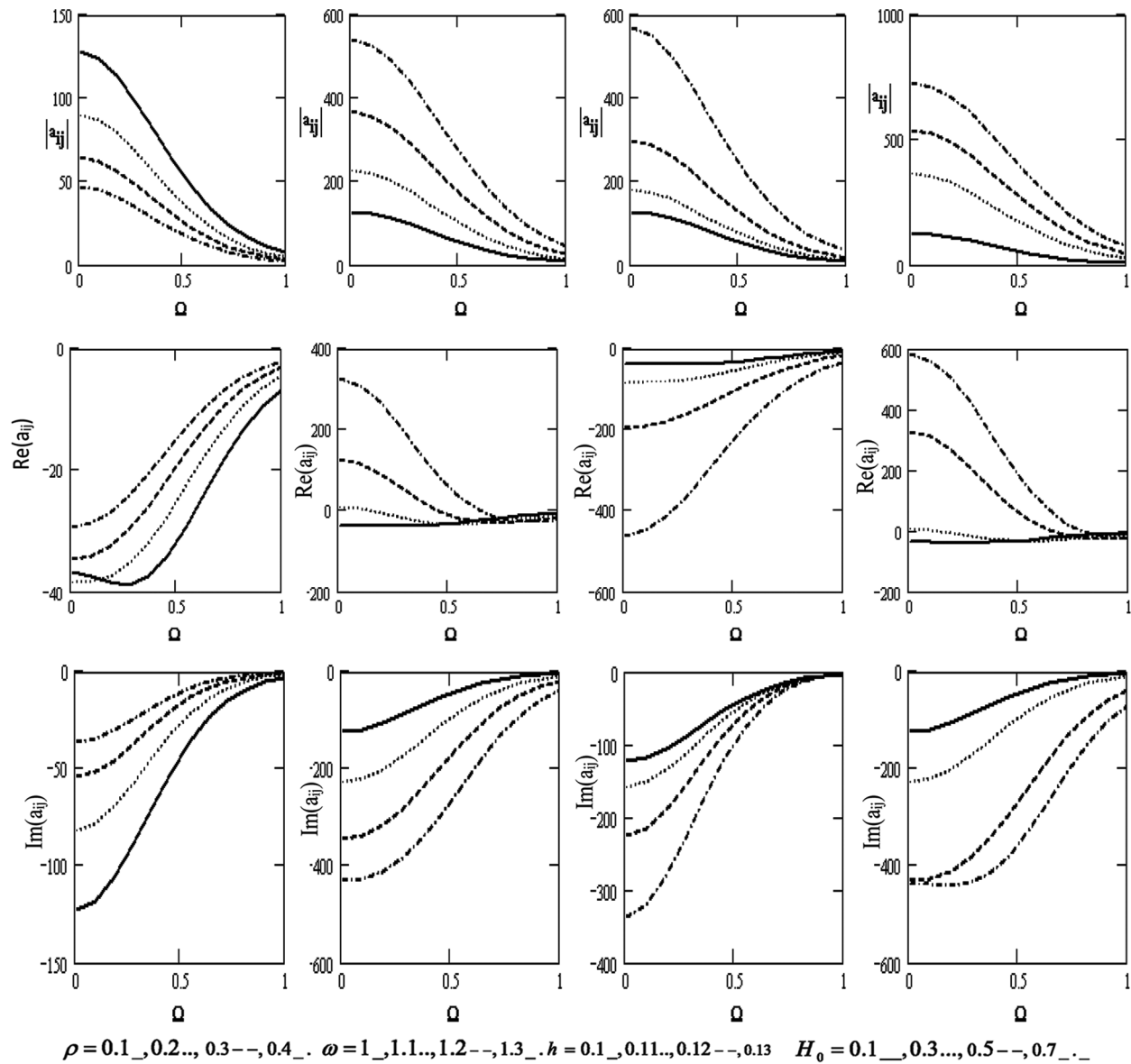
Figure 4: Variations of the determinant $|a_{ij}|$, $\text{Re}(a_{ij})$, $\text{Im}(a_{ij})$ ($i, j = 1,2,3,4$) with respect to the rotation Ω with different values for ρ, ω, h and H_0

5 Frequency Equation: Special Cases

5.1 Motion Independent of z

The frequency Eq. (20) degenerates into the product of two determinants

$$\Delta_1 \Delta_2 = 0$$

where

$$\Delta_1 = \begin{vmatrix} a_{11} & a_{12} & a_{13} & a_{15} & a_{16} & a_{17} \\ a_{21} & a_{22} & a_{23} & a_{25} & a_{26} & a_{27} \\ a_{41} & a_{42} & a_{43} & a_{45} & a_{46} & a_{47} \\ a_{51} & a_{52} & a_{53} & a_{55} & a_{56} & a_{57} \\ a_{61} & a_{62} & a_{63} & a_{65} & a_{66} & a_{67} \\ a_{81} & a_{82} & a_{83} & a_{85} & a_{86} & a_{87} \end{vmatrix} = 0, \qquad \Delta_2 = \begin{vmatrix} a_{34} & a_{38} \\ a_{74} & a_{78} \end{vmatrix} = 0. \tag{21}$$

The terms $a_{ij}(a)$ and $a_{ij}(b)$ appearing in Δ_1 and Δ_2 are given in Eq. (21) for the wavenumbers $k = 0$, α_1^2, α_2^2, α_3^2 are positive. Therefore, the Bessel functions of the first and second kinds are included in the solution. This equation could have been obtained immediately from the displacement equation of Eqs. (7) by setting $u_r = u_\theta = 0$, $\dfrac{\partial}{\partial z} = 0$ with the result:

$$(c_{44} + \mu_e H_0^2) \left[\frac{\partial^2 u_z}{\partial r^2} + r^{-1} \frac{\partial u_z}{\partial r} + r^{-2} \frac{\partial^2 u_z}{\partial \theta^2} \right] = \rho \left(\frac{\partial^2 u_z}{\partial t^2} - \Omega^2 \right) \tag{22}$$

5.2 Motion Independent of θ

If the motion becomes independent of the angular coordinate θ, the frequency Eq. (20) is declined to two determinants Δ_3, Δ_4 in the following form

$$\Delta_3 \Delta_4 = 0 \tag{23}$$

The terms a_{ij} in Δ_3 and Δ_4 are given by Eq. (23) for $n = 0$.

$$\Delta_3 = \begin{vmatrix} a_{11} & a_{12} & a_{13} & a_{15} & a_{16} & a_{17} \\ a_{21} & a_{22} & a_{23} & a_{25} & a_{26} & a_{27} \\ a_{31} & a_{32} & a_{33} & a_{35} & a_{346} & a_{37} \\ a_{51} & a_{52} & a_{53} & a_{55} & a_{56} & a_{57} \\ a_{61} & a_{62} & a_{63} & a_{65} & a_{66} & a_{67} \\ a_{71} & a_{72} & a_{73} & a_{75} & a_{76} & a_{77} \end{vmatrix} = 0, \qquad \Delta_4 = \begin{vmatrix} a_{44} & a_{48} \\ a_{84} & a_{88} \end{vmatrix} = 0. \tag{24}$$

Now, Eq. (23) is satisfied if $\Delta_3 = 0$ or $\Delta_4 = 0$. The case of $\Delta_3 = 0$ displays the equation of frequency of vibrations that are axially symmetric of an infinite hollow poroelastic cylinder.

5.3 Motion Independent of θ and z

If the wavenumbers k (for the infinite wavelength) $\lambda = \dfrac{2\pi}{k}$ and n disappear, the frequency equation declines into three uncoupled mode groups that can be defined as plane-strain extensional, longitudinal shear, and plane-strain shear. The equations of the frequency of the three types of motion take the following form

$$\Delta_5 \Delta_6 \Delta_7 = 0 \tag{25}$$

The terms a_{ij} in (25) are given by (20).

$$\Delta_5 = \begin{vmatrix} a_{13} & a_{15} \\ a_{53} & a_{55} \end{vmatrix} = 0, \ \Delta_6 = \begin{vmatrix} a_{44} & a_{48} \\ a_{84} & a_{88} \end{vmatrix} = 0, \ \Delta_7 = \begin{vmatrix} a_{34} & a_{38} \\ a_{74} & a_{78} \end{vmatrix} = 0. \tag{26}$$

$\rho = 0.1\_, 0.2.., 0.3--, 0.4\_.$ $\omega = 1\_, 1.1.., 1.2--, 1.3\_.$ $h = 0.1\_, 0.11.., 0.12--, 0.13$ $H_0 = 0.1\_\_, 0.3..., 0.5--, 0.7\_.\_$
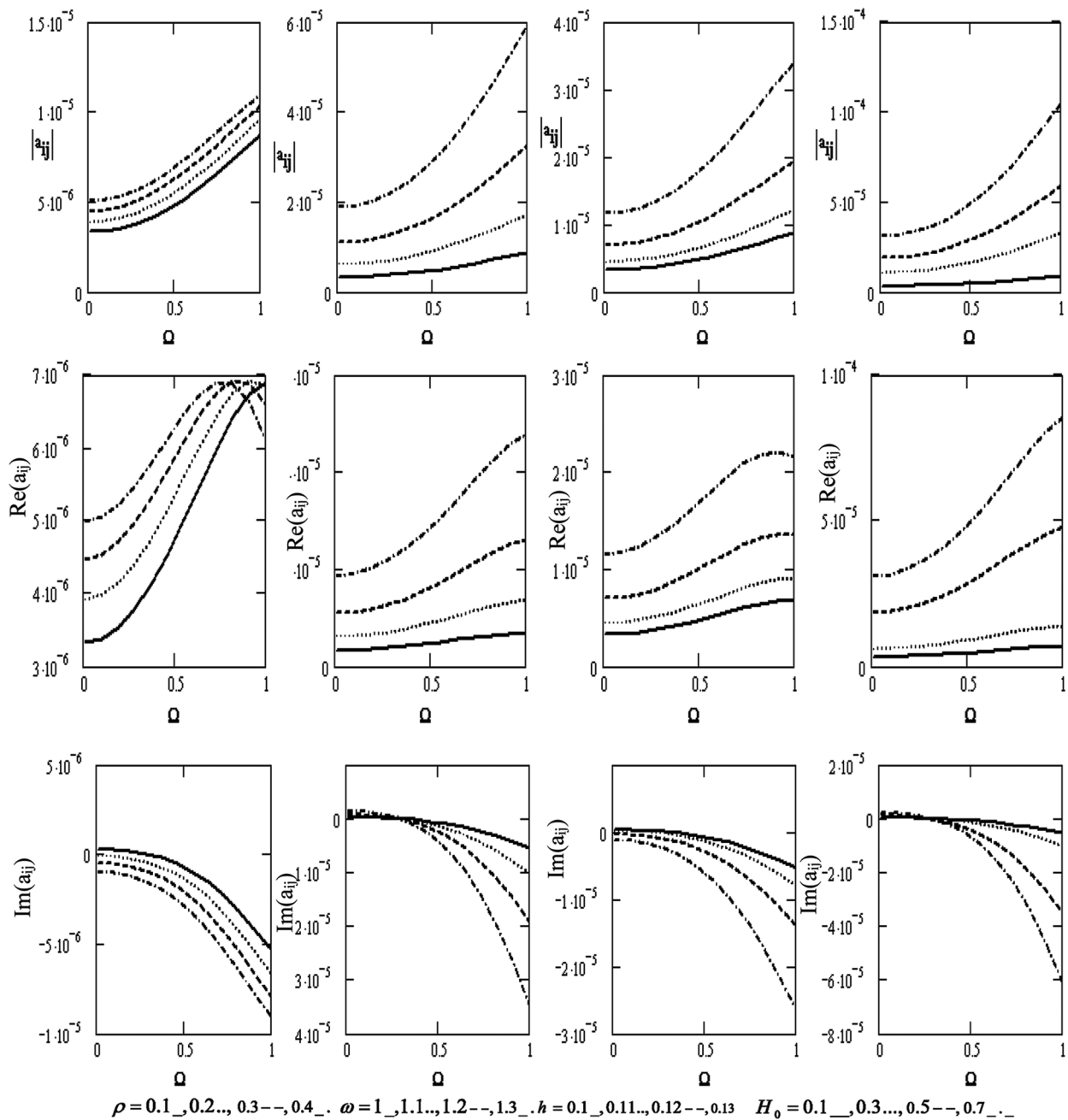
Figure 5: Variations of the determinant $|a_{ij}|$, $\mathrm{Re}(a_{ij})$, $\mathrm{Im}(a_{ij})$ $(i,j = 1,2,3,4)$ with respect to the rotation Ω with different values of ρ, ω, h and H_0 if the motion is independent of z

6 Numerical Results and Discussion

The numerical results of the equation of frequency are calculated for the wet bone. The roots are obtained for $n = 0$ and the longitudinal mode and flexural mode $n = 1, 2$. These findings are estimated within $0 < \varepsilon 1 < 4$ and $0 < ch < 4$. Based on [8], the elastic constant values of the bone are obtained and the poroelastic constant is estimated by the following form

$$Q = \frac{f(1 - f - \frac{\delta}{\chi})}{(\gamma + \delta + \frac{\delta^2}{\chi})}, \qquad R = \frac{f^2}{(\gamma + \delta + \frac{\delta^2}{\chi})},$$

where f is the porosity and γ, δ, χ are the Young's modulus and the Poisson ratio. The constants γ, δ, χ are

$$\chi = \frac{3(1 - 2v)}{E}, \quad \delta = 0.6\chi \quad and \quad \gamma = f(c - \delta)$$

where c is zero concerning the incompressibility fluid.

The human bone porosity within the age group 35–40 years is estimated as 0.24 [1]. To evaluate one more poroelastic constant, the following equation is defined $\frac{M}{Q} = \frac{c_{12}}{c_{13}}$ in which the value M is not given. Because the fluid is generally isotropic, $b_{rr} = b_{zz}$, the fluid density in the porospace, permeability of the medium, and mass density of the bone take the form of [15] as in Tab. 1.

Table 1: The constants of the material

c_{11}	c_{12}	c_{13}	c_{33}	c_{44}	a	b
2.12	0.95	1.02	3.76	0.75	0.8	1.4

Fig. 1 shows a considerable modification of the absolute value of $|\alpha_1|$, $|\alpha_2|$, $|\alpha_3|$ and $|\alpha_4|$ coefficients for the poroelastic bones concerning the rotation Ω that increases with increasing rotation for the diverse values of the density ρ, frequency ω, thickness h, and magnetic field H_0. It rises with an increase in the density, frequency, and magnetic field at the effect of density and the coefficients of $|\alpha_1|$, $|\alpha_3|$. It also increases and decreases with the increase of the density.

Fig. 2 displays various coefficients of $|d_1|$, $|d_2|$, $|d_3|$ and $|d_4|$ for the poroelastic bone concerning the rotation Ω, which increases with increasing the rotation for diverse values of the frequency ω, the thickness h, and the magnetic field H_0 except for the effect of the density because it increases and decreases. It declines with rising the frequency, thickness, and magnetic field except for the coefficient $|d_4|$ that rises with rising the density, frequency, and thickness. Moreover, the coefficients decrease with increasing the magnetic field.

Fig. 3 graphically portrays the variations of the absolute of the coefficients for the poroelastic bone of $|e_1|$, $|e_2|$, $|e_3|$ and $|e_4|$ concerning the rotation Ω. It rises with rising the rotation for diverse values of the density ρ, the frequency ω, the thickness, and the magnetic field H_0, while it rises with rising the density, frequency, and thickness except for the effect of the magnetic field. In this case, the absolute of the coefficients is the oscillatory behavior in the scope of the Ω-axis for the diverse values of the magnetic field.

Fig. 4 shows the variations of the scalar equation $|a_{ij}|$, wave velocity $\text{Re}(|a_{ij}|)$, and attenuation coefficient $\text{Im}(|a_{ij}|)$ concerning the rotation Ω for diverse values of the density ρ, the frequency ω, the thickness h, and the magnetic field H_0. It declines with the growing rotation. We also note that the scalar equation increases with the higher frequency, thickness, and magnetic field. On the contrary, it decreases with a higher density. Wave velocity increases with increasing density and rotation. It also rises with the higher frequency and magnetic field but decreases with higher rotation. It declines with higher thickness, and the attenuation coefficient declines with the higher frequency, thickness, magnetic field, and rotation, H_0. Additionally, wave velocity rises with higher rotation and density.
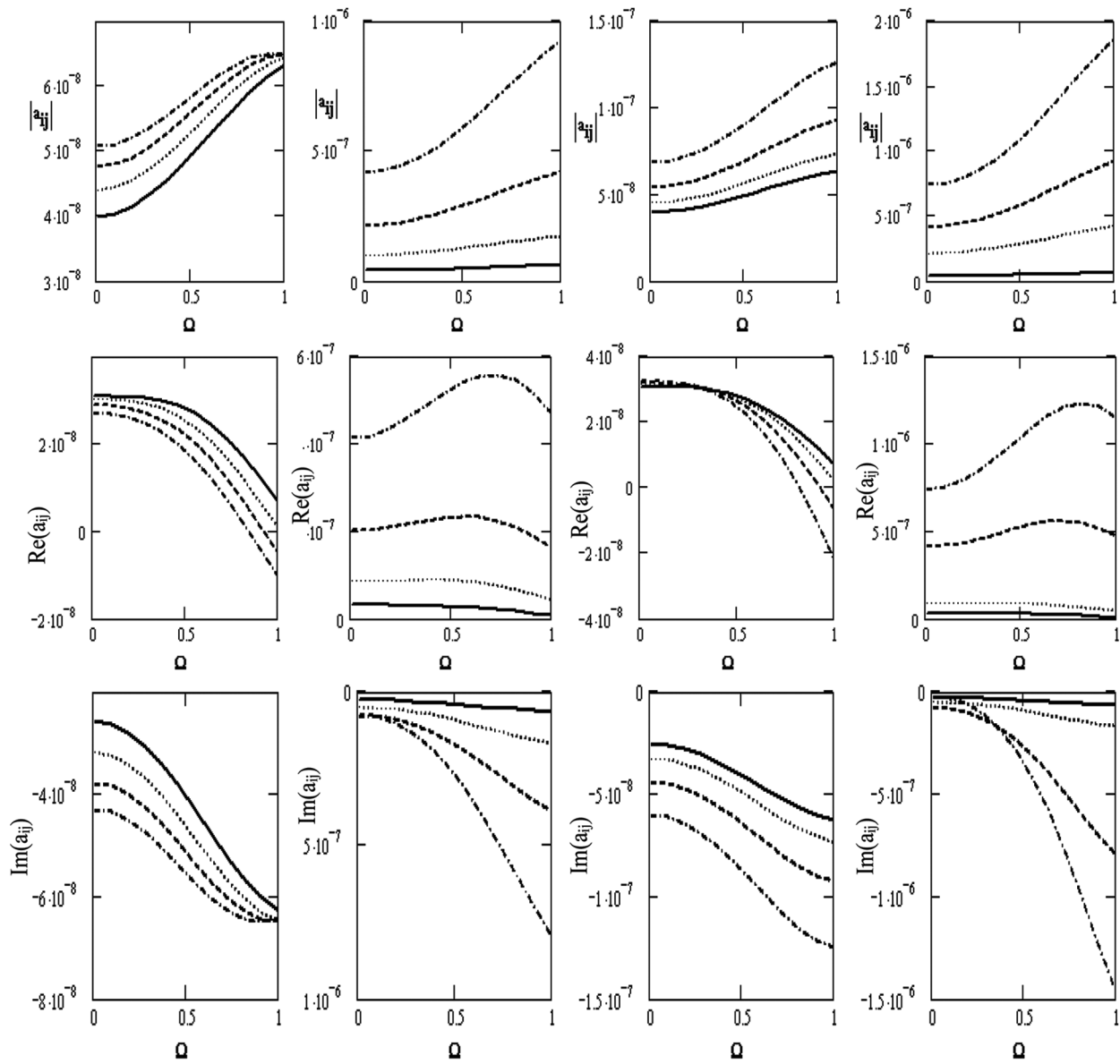
$\rho = 0.1\_, 0.2.., 0.3--, 0.4\_.$ $\omega = 1\_, 1.1.., 1.2--, 1.3\_.$ $h = 0.1\_, 0.11.., 0.12--, 0.13$ $H_0 = 0.1\_\_, 0.3..., 0.5--, 0.7\_\cdot\_$

Figure 6: Variations of the determinant $|a_{ij}|$, $\mathrm{Re}(a_{ij})$, $\mathrm{Im}(a_{ij})$ $(i,j = 1, 2, 3, 4)$ with respect to the rotation Ω with different values of ρ, ω, h and H_0 (if the motion is independent of θ)
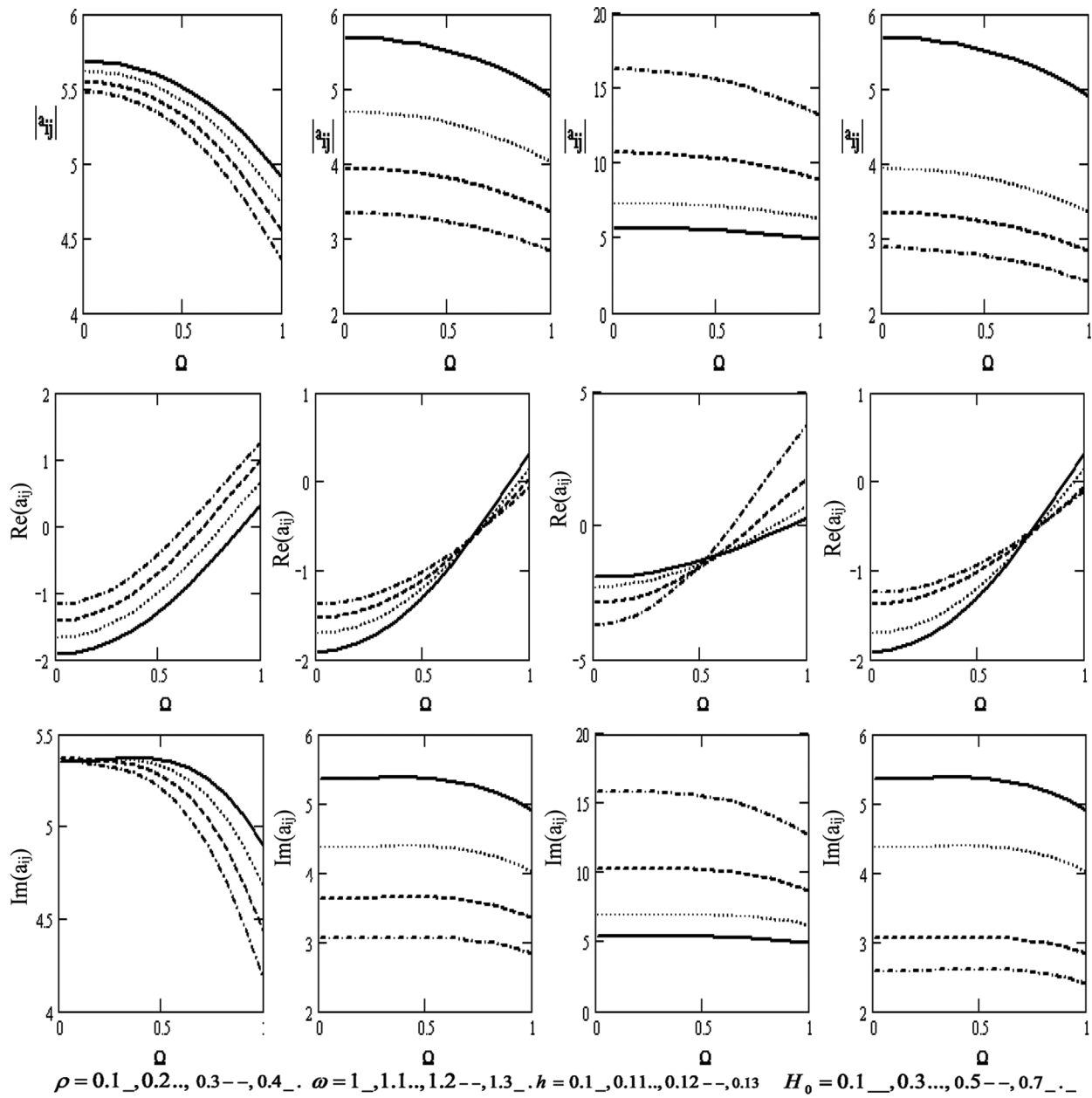
Figure 7: Variations of $|a_{ij}| = |\Delta_5||\Delta_7|$, $\text{Re}(|a_{ij}|)$, $\text{Im}(|a_{ij}|)$ with respect to the rotation Ω with different values of ρ, ω, h and H_0 (if the motion independent is of θ and z)

Fig. 5 graphically irradiates the effect of the variations of the scalar equation $|a_{ij}|$, the wave velocity $\text{Re}(|a_{ij}|)$, and the attenuation coefficients $\text{Im}(|a_{ij}|)$ concerning the rotation Ω for diverse values of the density ρ, the frequency ω, the thickness h, and the magnetic field H_0 (if the motion is independent of z). The scalar equation rises with higher density, frequency, thickness, magnetic, field, and rotation. Wave velocity rises with higher frequency, thickness, magnetic field, and rotation, except for the effect of the density that rises and declines with higher density. Attenuation coefficients decline with higher density, frequency, thickness, magnetic field, and rotation. They shift downward from positive to negative values.

Fig. 6 illustrates the variations of the scalar equation $|a_{ij}|$, the wave velocity $\text{Re}(|a_{ij}|)$, and the attenuation coefficients $\text{Im}(|a_{ij}|)$ concerning the rotation Ω for diverse values of the density ρ, the frequency ω, the thickness h, and the magnetic field H_0 (if the motion is independent of θ). The scalar equation rises with higher density, frequency, thickness, magnetic field, and rotation. Wave velocity rises with higher frequency and magnetic field, while it has an oscillatory with the x-axis. However, it declines with higher density, thickness, and rotation. Attenuation coefficients decrease with higher density, frequency, thickness, magnetic field, and rotation. They shift downward from positive to negative values.

Fig. 7 displays the variations of the scalar equation $|a_{ij}|$, the wave velocity $\text{Re}(|a_{ij}|)$, and the attenuation coefficients $\text{Im}(|a_{ij}|)$ concerning the rotation (if the motion is independent of θ and z) for the diverse values of the density ρ, the frequency ω, the thickness h, and the magnetic field H_0. The scalar equation decreases with higher density, frequency, magnetic field, and rotation but declines with higher thickness. Wave velocity rises with higher rotation, density, frequency, and magnetic field, except for the effect of thickness it declines with higher thickness. Moreover, the attenuation coefficient decreases with higher density, frequency, rotation, and magnetic field and rises with higher thickness.

7 Conclusion

In this paper, the wave propagation of a poroelastic bone with a circular cylindrical cavity subjected to the rotation and the magnetic field is considered. The frequency equation is obtained by considering the material as transversely isotropic in nature. The numerical results are obtained and compared for the bone in the presence and absence of the magnetic field and the rotation. The findings of the study can be useful for the applications of the poroelastic materials in the orthopedics, the dental, and the cardiovascular fields are well known. The results obtained have significant applications related to medicine, chemical engineering, and orthopedics surgery.

Conflicts of Interest: The authors declare that there are no conflicts of interest between all authors.

References

[1] A. N. Natall and E. A. Meroi, "A review of the biomechanical properties of bone as a material," *Journal of Biomedical Engineering*, vol. 11, pp. 266–277, 1986.

[2] S. M. Ahmed and A. M. Abd-Alla, "Electromechanical wave propagation in a cylindrical poroelastic bone with cavity," *Applied Mathematics and Computation*, vol. 133, no. 2–3, pp. 257–286, 2002.

[3] A. M. El-Naggar, A. M. Abd-Alla and S. R. Mahmoud, "Analytical solution of electro-mechanical wave propagation in longbones," *Applied Mathematics and Computation*, vol. 119, no. 1, pp. 77–98, 2001.

[4]   A. M. Abd-Alla, S. M. Abo-Dahab and S. R. Mahmoud, "Wave propagation modeling in cylindrical human long wet boneswith cavity," *Meccanica*, vol. 46, no. 6, pp. 1413–1428, 2011.

[5]   A. M. Abd-Alla and S. M. Abo-Dahab, "Effect of magnetic field on poroelastic bone model for internal remodeling," *Applied Mathematics and Mechanics*, vol. 34, no. 7, pp. 889–906, 2013.

[6]   S. M. Abo-Dahab, A. M. Abd-Alla and S. Alqosami, "Effect of rotation on wave propagation in hollow poroelastic circular cylinder," *Mathematical Problems in Engineering*, vol. 2014, no. 7, pp. 16, 2014.

[7]   A. M. Abd-Alla and G. A. Yahya, "Wave propagation in a cylindrical human long wet bone," *Journal of Computational and Theoretical Nanoscience*, vol. 10, no. 3, pp. 750–755, 2013.

[8]   M. A. Biot, "Theory of elasticity and consolidation for a porous anisotropic solid," *Journal of Applied Physics*, vol. 26, no. 2, pp. 182–185, 1955.

[9]   M. A. Biot, "Theory of propagation of elastic waves in a fluid-saturated porous solid I: Low-frequency range," *Acoustical Society of America*, vol. 28, no. 2, pp. 168–178, 1956.

[10] L. Cardoso and S. C. Cowin, "Role of structural anisotropy of biological tissues in poroelastic wave propagation," *Mechanics of Materials*, vol. 44, pp. 174–188, 2012.

[11] P. J. Matuszyk and L. F. Demkowicz, "Solution of coupled poroelastic/acoustic/elastic wave propagation problems using automatic hp-adaptivity," *Computer Methods in Applied Mechanics and Engineering*, vol. 281, pp. 54–80, 2014.

[12] P. H. Wen, "Meshless local Petrov–Galerkin (MLPG) method for wave propagation in 3D poroelastic solids," *Engineering Analysis with Boundary Elements*, vol. 34, no. 4, pp. 315–323, 2010.

[13] C. Morin and C. Hellmich, "A multiscale poromicromechanical approach to wave propagation and attenuation in bone," *Ultrasonics*, vol. 54, no. 5, pp. 1251–1269, 2014.

[14] V. T. Potsika, K. N. Grivas, V. C. Protopappas, M. G. Vavva, K. Raum *et al.*, "Application of an effective medium theory for modeling ultrasound wave propagation in healing long bones," *Ultrasonics*, vol. 54, no. 5, pp. 1219–1230, 2014.

[15] V. A. Papathanasopoulou, D. I. Fotiadis, G. Foutsitzi and C. V. Massalas, "A poroelastic bone model for internal remodeling," *International Journal of Engineering Science*, vol. 40, no. 5, pp. 511–530, 2002.

[16] V. H. Nguyen, T. Lemaire and S. Naili, "Poroelastic behaviour of cortical bone under harmonic axial loading: A finite element study at the osteonal scale," *Medical Engineering & Physics*, vol. 32, no. 4, pp. 384–390, 2010.

[17] J. C. Misra and S. C. Samanta, "Wave propagation in tubular bones," *International Journal of Solids and Structures*, vol. 20, no. 1, pp. 55–62, 1984.

[18] Q. H. Qin, C. Qu and J. Ye, "Thermoelectroelastic solutions for surface bone remodeling under axial and transverse loads," *Biomaterials*, vol. 26, no. 33, pp. 6798–6810, 2005.

[19] V. Mathieu, R. Vayron, G. Richard, G. Lambert, S. Naili *et al.*, "Biomechanical determinants of the stability of dental implants: Influence of the bone-implant interface properties," *Journal of Biomechanics*, vol. 47, no. 1, pp. 3–13, 2014.

[20] T. Brynk, C. Hellmich, A. Fritsch, P. Zysset and J. Eberhardsteiner, "Experimental poromechanics of trabecular bone strength: Role of Terzaghi's effective stress and of tissue level stress fluctuations," *Journal of Biomechanics*, vol. 44, no. 3, pp. 501–508, 2011.

[21] W. J. Parnell, M. B. Vu, Q. Grimal and S. Naili, "Analytical methods to determine the effective mesoscopic and macroscopic elastic properties of cortical bone," *Biomechanics and Modeling in Mechanobiology*, vol. 11, no. 6, pp. 883–901, 2012.

[22] A. Shah, "Flexural wave propagation in coated poroelastic cylinders with reference to fretting fatigue," *Journal of Vibration and Control*, vol. 17, no. 7, pp. 1049–1064, 2011.

[23] R. P. Gilbert, P. Guyenne and M. Y. Ou, "A quantitative ultrasound model of the bone with blood as the interstitial fluid," *Mathematical and Computer Modelling*, vol. 55, no. 9–10, pp. 2029–2039, 2012.

[24] L. Cui, A. H. D. Cheng and Y. Abousleiman, "Poroelastic solutions of an inclined borehole," *Transactions of ASME, Journal of Applied Mechanics*, vol. 64, no. 1, pp. 32–38, 1997.

[25] S. C. Cowin, "Bone poroelasticity," *Journal of Biomechanics*, vol. 32, no. 3, pp. 217–238, 1999.

[26] V. Mathieu, R. Vayron, E. Soffer and F. Anagnostou, "Influence of healing time on the ultrasonic response of the bone-implant interface," *Ultrasound in Medicine & Biology*, vol. 38, no. 4, pp. 611–618, 2012.

[27] A. Singhal, S. A. Sahu and S. Chaudhary, "Study of surface wave vibration in rotating human long bones of cylindrical shape under the magnetic field influence," *Waves in Random and Complex Media*, vol. 37, no. 2, pp. 1–17, 2019.

[28] R. Kumhar, S. Kundu, M. Maity and S. Gupta, "Mechanical waves study in tri-materials bars having sinusoidally interfaces (i.e. Fiber-reinforced, Poroelastic and Isotropic)," *Materials Research Express*, vol. 6, no. 12, pp. 125335, 2019.

[29] S. M. Abo-Dahab, A. M. Abd-Alla, S. Alqosami and H. S. Gafel, "Analytical solution for surface waves remodeling in long bones under rotating and magnetic field," *JP Journal of Heat and Mass Transfer*, vol. 20, no. 1, pp. 1–30, 2020.

[30] A. M. Farhan, "Effect of rotation on the propagation of waves in hollow poroelastic circular cylinder with magnetic field," *Computers, Materials & Continua*, vol. 53, no. 2, pp. 129–156, 2017.

[31] M. Marin, A. M. Abd-Alla, D. Raducanu and M. S. Abo-Dahab, "Structural continuous dependence in micropolar porous bodies," *Computers, Materials & Continua*, vol. 45, no. 2, pp. 107–125, 2015.

[32] S. M. Abo-Dahab, A. M. Abd-Alla, J. Bouslimi and M. Omri, "Effect of rotation on waves propagation model in a human long poroelastic bone. submitted for publication, 2020.

Appendix

$$a_{11} = [(\overline{c}_{11} + \mu_e H_0^2)(\frac{n^2}{\alpha_1^2 \overline{a}^2} - \frac{n}{\alpha_1 \overline{a}} - 1)J_n(\alpha_1 \overline{a}) + ((\frac{n}{\alpha_1 \overline{a}} - \frac{n^2}{\overline{a}^2})J_n(\alpha_1 \overline{a}) + \frac{1}{\alpha_1 \overline{a}}J_{n+1}(\alpha_1 \overline{a}) -$$

$$- \frac{1}{\overline{a}}(\overline{c}_{11} + \mu_e H_0^2)J_{n+1}(\alpha_1 \overline{a}) - \varepsilon_1 d_1(\overline{c}_{13} + \mu_e H_0^2)J_n(\alpha_1 \overline{a}) + (\frac{n^2}{\alpha_1^2 \overline{a}^2} - \frac{n^2}{\overline{a}^2} - 1)J_n(\alpha_1 \overline{a}) + (\frac{1}{\alpha_1 \overline{a}} -$$

$$- \frac{1}{\overline{a}})J_{n+1}(\alpha_1 \overline{a})\overline{M}],$$

$$a_{12} = [((\frac{n^2}{\alpha_2^2 \overline{a}^2} - \frac{n}{\alpha_2 \overline{a}} - 1)J_n(\alpha_2 \overline{a}) + \frac{1}{\alpha_2 \overline{a}}(\overline{c}_{11} + \mu_e H_0^2)J_n(\alpha_2 \overline{a}) +$$

$$+ (\frac{n}{\alpha_2 \overline{a}} - \frac{n^2}{\overline{a}^2})J_n(\alpha_2 \overline{a}) - \frac{1}{\overline{a}}(\overline{c}_{12} + \mu_e H_0^2)J_{n+1}(\alpha_2 \overline{a}) - \varepsilon_1 d_2(\overline{c}_{13} + \mu_e H_0^2)J_{n+1}(\alpha_2 \overline{a}) +$$

$$+ ((\frac{n^2}{\alpha_2^2 \overline{a}^2} - \frac{n^2}{\overline{a}^2} - 1)J_n(\alpha_2 \overline{a}) + +(\frac{1}{\alpha_2 \overline{a}} - \frac{1}{\overline{a}})J_{n+1}(\alpha_2 \overline{a})\overline{M}],$$

$$a_{13} = [(\overline{c}_{11} + \mu_e H_0^2)(\frac{n^2}{\alpha_3^2 \overline{a}^2} - \frac{n}{\alpha_3 \overline{a}} - 1)J_n(\alpha_3 \overline{a}) + ((\frac{n}{\alpha_3 \overline{a}} - \frac{n^2}{\overline{a}^2})J_n(\alpha_3 \overline{a}) + \frac{1}{\alpha_3 \overline{a}}J_{n+1}(\alpha_3 \overline{a}) -$$

$$- \frac{1}{\overline{a}}(\overline{c}_{11} + \mu_e H_0^2)J_{n+1}(\alpha_3 \overline{a}) - \varepsilon_1 d_1(\overline{c}_{13} + \mu_e H_0^2)J_n(\alpha_3 \overline{a}) + (\frac{n^2}{\alpha_1^2 \overline{a}^2} - \frac{n^2}{\overline{a}^2} - 1)J_n(\alpha_3 \overline{a}) + (\frac{1}{\alpha_3 \overline{a}} -$$

$$- \frac{1}{\overline{a}})J_{n+1}(\alpha_3 \overline{a})\overline{M}],$$

$$a_{14} = \frac{n}{\overline{a}}(\overline{c}_{11} - \overline{c}_{12})[-\alpha_4 J_{n+1}(\alpha_4 \overline{a}) + \frac{(n+1)}{\overline{a}}J_n(\alpha_4 \overline{a}),$$

$$a_{15} = [(\overline{c}_{11} + \mu_e H_0^2)(\frac{n^2}{\alpha_1^2 \overline{a}^2} - \frac{n}{\alpha_1 \overline{a}} - 1)Y_n(\alpha_1 \overline{a}) + ((\frac{n}{\alpha_1 \overline{a}} - \frac{n^2}{\overline{a}^2})Y_n(\alpha_1 \overline{a}) + \frac{1}{\alpha_1 \overline{a}}Y_{n+1}(\alpha_1 \overline{a}) -$$

$$- \frac{1}{\overline{a}}(\overline{c}_{11} + \mu_e H_0^2)Y_{n+1}(\alpha_1 \overline{a}) - \varepsilon_1 d_1(\overline{c}_{13} + \mu_e H_0^2)Y_n(\alpha_1 \overline{a}) + (\frac{n^2}{\alpha_1^2 \overline{a}^2} - \frac{n^2}{\overline{a}^2} - 1)Y_n(\alpha_1 \overline{a}) + (\frac{1}{\alpha_1 \overline{a}} -$$

$$- \frac{1}{\overline{a}})J_{n+1}(\alpha_1 \overline{a})\overline{M}],$$

$$a_{16} = [((\frac{n^2}{\alpha_2^2 \overline{a}^2} - \frac{n}{\alpha_2 \overline{a}} - 1)Y_n(\alpha_2 \overline{a}) + \frac{1}{\alpha_2 \overline{a}}(\overline{c}_{11} + \mu_e H_0^2)Y_n(\alpha_2 \overline{a}) +$$

$$+ (\frac{n}{\alpha_2 \overline{a}} - \frac{n^2}{\overline{a}^2})Y_n(\alpha_2 \overline{a}) - \frac{1}{\overline{a}}(\overline{c}_{12} + \mu_e H_0^2)Y_{n+1}(\alpha_2 \overline{a}) - \varepsilon_1 d_2(\overline{c}_{13} + \mu_e H_0^2)Y_{n+1}(\alpha_2 \overline{a}) +$$

$$+ ((\frac{n^2}{\alpha_2^2 \overline{a}^2} - \frac{n^2}{\overline{a}^2} - 1)Y_n(\alpha_2 \overline{a}) + +(\frac{1}{\alpha_2 \overline{a}} - \frac{1}{\overline{a}})Y_{n+1}(\alpha_2 \overline{a})\overline{M}],$$

$$a_{17} = [(\overline{c}_{11} + \mu_e H_0^2)(\frac{n^2}{\alpha_3^2 \overline{a}^2} - \frac{n}{\alpha_3 \overline{a}} - 1)Y_n(\alpha_3 \overline{a}) + ((\frac{n}{\alpha_3 \overline{a}} - \frac{n^2}{\overline{a}^2})Y_n(\alpha_3 \overline{a}) + \frac{1}{\alpha_3 \overline{a}}Y_{n+1}(\alpha_3 \overline{a}) -$$

$$- \frac{1}{\overline{a}}(\overline{c}_{11} + \mu_e H_0^2)Y_{n+1}(\alpha_3 \overline{a}) - \varepsilon_1 d_1(\overline{c}_{13} + \mu_e H_0^2)Y_n(\alpha_3 \overline{a}) + (\frac{n^2}{\alpha_1^2 \overline{a}^2} - \frac{n^2}{\overline{a}^2} - 1)Y_n(\alpha_3 \overline{a}) + (\frac{1}{\alpha_3 \overline{a}} -$$

$$- \frac{1}{\overline{a}})Y_{n+1}(\alpha_3 \overline{a})\overline{M}],$$

$$a_{18} = \frac{n}{\overline{a}}(\overline{c}_{11} - \overline{c}_{12})[-\alpha_4 Y_{n+1}(\alpha_4 \overline{a}) + \frac{(n+1)}{\overline{a}}Y_n(\alpha_4 \overline{a}),$$

$$a_{21} = [\frac{2n}{\overline{a}}(-\alpha_1 J_{n+1}(\alpha_1 \overline{a}) + \frac{(n-1)}{\overline{a}}J_n(\alpha_1 \overline{a}))], \quad a_{22} = [\frac{2n}{\overline{a}}(-\alpha_2 J_{n+1}(\alpha_1 \overline{a}) + \frac{(n-1)}{\overline{a}}J_n(\alpha_2 \overline{a}))],$$

$$a_{23} = [\frac{2n}{\overline{a}}(-\alpha_3 J_{n+1}(\alpha_3 \overline{a}) + \frac{(n-1)}{\overline{a}}J_n(\alpha_3 \overline{a}))],$$

$$a_{24} = (\frac{1}{\overline{a}})^2[2\overline{a}\alpha_4 J_{n+1}(\overline{a}\alpha_4) + (\alpha_4^2 \overline{a}^2 + 2n^2 - 2n)J_n(\overline{a}\alpha_4)],$$

$$a_{25} = [\frac{2n}{\overline{a}}(-\alpha_1 Y_{n+1}(\alpha_1 \overline{a}) + \frac{(n-1)}{\overline{a}}Y_n(\alpha_1 \overline{a}))], \quad a_{26} = [\frac{2n}{\overline{a}}(-\alpha_2 Y_{n+1}(\alpha_1 \overline{a}) + \frac{(n-1)}{\overline{a}}Y_n(\alpha_2 \overline{a}))],$$

$$a_{27} = [\frac{2n}{\overline{a}}(-\alpha_3 Y_{n+1}(\alpha_3 \overline{a}) + \frac{(n-1)}{\overline{a}}Y_n(\alpha_3 \overline{a}))],$$

$$a_{28} = (\frac{1}{\overline{a}})^2[2\overline{a}\alpha_4 Y_{n+1}(\overline{a}\alpha_4) + (\alpha_4^2 \overline{a}^2 + 2n^2 - 2n)Y_n(\overline{a}\alpha_4)],$$

$$a_{31} = \alpha_1(d_1 + \varepsilon_1)[\frac{n}{\overline{a}\alpha_1}J_n(\overline{a}\alpha_1) - J_{n+1}(\overline{a}\alpha_1)], \quad a_{32} = \alpha_2(d_2 + \varepsilon_1)[\frac{n}{\overline{a}\alpha_2}J_n(\overline{a}\alpha_2) - J_{n+1}(\overline{a}\alpha_2)],$$

$$a_{32} = \alpha_3(d_2 + \varepsilon_1)[\frac{n}{\overline{a}\alpha_2}J_n(\overline{a}\alpha_3) - J_{n+1}(\overline{a}\alpha_3)],$$

$$a_{34} = \frac{n}{\overline{a}} J_n(\overline{a}\alpha_4), \quad a_{35} = \alpha_1(d_1 + \varepsilon_1)[\frac{n}{\overline{a}\alpha_1} Y_n(\overline{a}\alpha_1) - Y_{n+1}(\overline{a}\alpha_1)],$$

$$a_{36} = \alpha_2(d_2 + \varepsilon_1)[\frac{n}{\overline{a}\alpha_2} Y_n(\overline{a}\alpha_2) - Y_{n+1}(\overline{a}\alpha_2)], \quad a_{37} = \alpha_3(d_2 + \varepsilon_1)[\frac{n}{\overline{a}\alpha_2} Y_n(\overline{a}\alpha_3) - Y_{n+1}(\overline{a}\alpha_3)],$$

$$a_{38} = \frac{n}{\overline{a}} Y_n(\overline{a}\alpha_4),$$

$$a_{41} = (\overline{M} - \frac{Q'e_1}{k^2} + \frac{R'e_1}{k^2})[(\frac{n^2}{\alpha_1^2\overline{a}^2} - \frac{n^2}{\overline{a}^2} - 1)J_n(\overline{a}\alpha_1) + (\frac{1}{\alpha_1\overline{a}} - \frac{1}{\overline{a}})J_{n+1}(\overline{a}\alpha_1),$$

$$a_{42} = (\overline{M} - \frac{Q'e_2}{k^2} + \frac{R'e_2}{k^2})[(\frac{n^2}{\alpha_2^2\overline{a}^2} - \frac{n^2}{\overline{a}^2} - 1)J_n(\overline{a}\alpha_2) + (\frac{1}{\alpha_2\overline{a}} - \frac{1}{\overline{a}})J_{n+1}(\overline{a}\alpha_2),$$

$$a_{43} = (\overline{M} - \frac{Q'e_3}{k^2} + \frac{R'e_3}{k^2})[(\frac{n^2}{\alpha_3^2\overline{a}^2} - \frac{n^2}{\overline{a}^2} - 1)J_n(\overline{a}\alpha_3) + (\frac{1}{\alpha_3\overline{a}} - \frac{1}{\overline{a}})J_{n+1}(\overline{a}\alpha_3),$$

$$a_{44} = 0, \quad a_{45} = (\overline{M} - \frac{Q'e_1}{k^2} + \frac{R'e_1}{k^2})[(\frac{n^2}{\alpha_1^2\overline{a}^2} - \frac{n^2}{\overline{a}^2} - 1)Y_n(\overline{a}\alpha_1) + (\frac{1}{\alpha_1\overline{a}} - \frac{1}{\overline{a}})Y_{n+1}(\overline{a}\alpha_1),$$

$$a_{46} = (\overline{M} - \frac{Q'e_2}{k^2} + \frac{R'e_2}{k^2})[(\frac{n^2}{\alpha_2^2\overline{a}^2} - \frac{n^2}{\overline{a}^2} - 1)Y_n(\overline{a}\alpha_2) + (\frac{1}{\alpha_2\overline{a}} - \frac{1}{\overline{a}})Y_{n+1}(\overline{a}\alpha_2),$$

$$a_{47} = (\overline{M} - \frac{Q'e_3}{k^2} + \frac{R'e_3}{k^2})[(\frac{n^2}{\alpha_3^2\overline{a}^2} - \frac{n^2}{\overline{a}^2} - 1)Y_n(\overline{a}\alpha_3) + (\frac{1}{\alpha_3\overline{a}} - \frac{1}{\overline{a}})Y_{n+1}(\overline{a}\alpha_3), \quad a_{48} = 0,$$

The remaining four rows can be obtained from the above equations by replacing $\overline{a}$ by $\overline{b}$.